Mohamed F. Atia[1], *Kamal Shalabi*[2], *Mohamed A. Ismail*[2], *Magdy. Abd El-Khalek*[2], *Abd El-Aziz S. Fouda*[2]*

[1]*Institute of aviation engineering and technology, Cairo, Egypt*
[2]*Department of Chemistry, Faculty of Science, Mansoura University, Mansoura 35516, Egypt*

Scientific paper
ISSN 0351-9465, E-ISSN 2466-2585
https://doi.org/10.62638/ZasMat1269

Zastita Materijala 66 ( )
(2025)

Contribution to the corrosion inhibition of carbon steel by 5-(2-ethoxybenzylidene) 1,3-dimethylbarbituric acid in HCl solution: Experimental and theoretical study

ABSTRACT

The inhibiting impact of ecofriendly 5-(2-ethoxybenzylidene) 1,3-dimethylbarbituric acid (5-EBMB) in 1 M HCl on the corrosion of C-steel has been examined via weight loss (WL) method, potentiodynamic polarization (PDP), electrochemical impedance spectroscopy (EIS), electrochemical frequency modulation (EFM) techniques”. The obtained results demonstrate that the studied chemical is good 5-EBMB and that, in both PDP and EIS methods, its inhibition efficiency (%IE) increases with increasing concentration, reaching 82.5 at $21x10^{-6}$ *M. Conversely, when the temperature rose, the percentage of IE reduced. “The adsorption of the investigated derivative on the surface of C-steel follows Langmuir isotherm. The adsorption process of the investigated compound is spontaneous and considered as chemisorption type”. PDP curves revealed that the studied derivative is mixed-type inhibitor. Furthermore, the EIS results verified that the compound under investigation had adsorbed on the C-steel surface by raising the charge transfer resistance (*R_{ct}*) to 139.7 ohm cm*^{2} *and decreasing the double layer (*C_{dl}*) capacitance from 102 to 69 µF cm*$^{-2}$*. The inhibitor adsorption on the C-steel surface was confirmed by surface examination using atomic force microscopy (AFM), energy dispersive X-ray (EDX), and scanning electron microscopy (SEM). Additionally, quantum chemistry and molecular dynamic simulation were used to extensively examine the mechanism of 5-EBMB's corrosion inhibition. All tested methods gave good agreement.*

Keywords*: Corrosion inhibition, HCl, C-steel, Arylidene barbituric acid derivative, Langmuir isotherm*

1. INTRODUCTION

Acidic media are generally applied for elimination of unwanted scale and corrosion in several industrial procedures. By monitoring metal dissolution attributable to acidic exposure, so 5-EBMBs are commonly applied within this operation [1]. “Organic 5-EBMBs today do the inhibition of corrosion well than the inorganic 5-EBMBs [2]. Organic compounds are kind of acidic 5-EBMBs including hetero atoms for example oxygen , sulfur, and nitrogen. Amongst, organic 5-EBMBs have several advantages for instance low cost, low poisonousness, high inhibition efficiency, and easy to organize” [3-6].

Generally, “heterocyclic organic compounds are applied to the corrosion inhibition on Cu [7] Al [8-10], Fe[11-16] and also other metals [17-18] within diverse corrosion media”. “A review of the literature on acid corrosion 5-EBMBs reveal that they work by adsorbing to the metal's surface. This effect may be caused by (i) electrostatic attraction between the charged metal and the charged 5-EBMB molecules, (ii) dipole-type interaction between uncharged electron pairs in the 5-EBMB and the metal, (iii) electron-interaction with the metal, or (iv) A combination of the aforementioned” [19]. Pyrimidine is a six-membered heterocyclic aromatic compound with two nitrogen atoms at positions 1 and 3. The chemistry of pyrimidine derivatives is crucial in medicine, agrochemicals, and a variety of biological activities. “Many well-known commercial medications contain pyrimidine derivatives, such as Uramustine, Piritrexim, Isetionate, Tegafur, Floxuridine, Fluorouracil,

---

*Corresponding author: Abd El-Aziz S. Fouda
E-mail: asfouda@mans.edu.eg
Paper received: 30.09.2024..
Paper accepted: 20.11.2024.
ORCID:0000-0002-3239-4417

Cytarabine, and Methotrexate. Furthermore, the pyrimidine skeleton is found in a wide range of natural products, including nucleic acids, vitamins, enzymes, chlorophyll, hemoglobin, and hormones". Ansari el al [20] "investigates the corrosion protection of mild steel by four PPDs in 1 M HCl solution and they found the percentage inhibition efficacy 88-97.1% at 400 mg L^{-1}. Numerous pyrimidine derivatives have been synthesized and studied their suitability for corrosion inhibition of variety of steel samples in acidic medium" [21-27]. "The efficacy of the organic compounds including hetero atoms as corrosion 5-EBMBs in acidic solutions for C-steels is well recognized" [28-32]. "Pyrimidines and their derivatives are important because they are available in nature, particularly in the nucleobases present in nucleic acids, and many of them have been discovered to be beneficial in chemotherapy" [33]."Currently in use as anticancer, antifungal, and antibacterial medicines are pyrimidine-containing chemotherapeutics" [34]. "Furthermore, in HCl and H_2SO_4 solutions, several pyrimidine derivatives were found to be efficient corrosion inhibitors for steel" [35]. Novel cationic and non-ionic biopolyurethanes for effective inhibition of mild steel corrosion in H_2S-CO_2 environment was studied by Banan, and Asadi [36], Haruna et al [37] reported the effect of acrylic acid modified indapamide-based polymer as an effective inhibitor against carbon steel corrosion in CO_2-saturated NaCl with variable H_2S levels. Bairagi et al [38] studied the effect of polymers and their composites for corrosion inhibition application

The purpose of this work is to study the impact of 5-(2-ethoxybenzylidene)-1,3-dimethylbarbituric (5-EBMB) acid as ecofriendly inhibitor for C-steel in 1 M hydrochloric acid solution by applying WL, PDP, EIS, EFM tests. The investigated 5-EBMB is not reported as a corrosion inhibitor for steel in the literatures before".

2. MATERIALS AND METHODS

"Chemical composition of C-steel coupons in weight percentage is: carbon (0.200); manganese (0.350); phosphorus (0.024); chromium; sulfur (0.003); and balance Fe".

"5-(2-Ethoxybenzylidene)-1,3-imethylbarbituric acid (5-EBMB) was prepared as outlined in scheme 1. The detailed information of 5-EBMB is reported in the literature" [39, 40] with identical melting point of 165-166ºC. 5-EBMB: Adopting the same methodology used for preparation before [40], starting with 2-ethoxybenzaldehyde instead of 4-methoxybenzaldehyde. "Yield 85%, mp 165–166 °C. IR (KBr) ν' 3114, 3095, 2987, 2950, 2900 (CH), 1730, 1670 (CO), 1577, 1541 (C=C) cm^{-1}"." ^1H NMR ($CDCl_3$); δ 1.37 (t, J = 7.2 Hz, 3H), 3.28 (s, 3H), 3.35 (s, 3H), 4.07 (q, J = 7.2 Hz, 2H), 6.84 (d, J = 8.4 Hz, 1H), 6.92 (t, J = 7.2 Hz, 1H), 7.39 (t, J = 7.2 Hz, 1H), 7.98 (d, J = 8.4 Hz, 1H), 8.85 (s, 1H)". "MS (EI) m/e (rel.int.); 288 (M^+, 24), 243 (100).Anal. Calc. for $C_{15}H_{16}N_2O_4$ (288.30): C, 62.49; H, 5.59; N, 9.72. Found. C, 62.21; H, 5.73; N, 9.48"

Table 1. Chemical structures of tested 5-EBMB inhibitor

Molecular structures/Chemical name
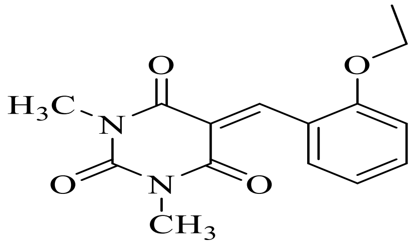 5-(2-Ethoxybenzylidene)-1,3-dimethylbarbituric acid (5-EBMB)
Chemical Formula $C_{15}H_{16}N_2O_4$, Molecular Weight 288.3

The aggressive solutions used were prepared from analytical grade HCl. A 1M HCl solution was prepared using bidistilled water, both with and without different concentrations of inhibitor. All experiments were conducted in stagnant, aerated solutions.

2.1. WL method

"Samples used in weight loss measurements were coupons measuring 2 cm x 2 cm x 0.2 cm. Before starting any experiment, specimens were prepared by abrading them successively with emery paper (grades 100–1200), followed by thorough washing with bidistilled water, degreasing with acetone, and drying in a stream of air. The weight loss method involved the following steps: Each coupon was weighed using an analytical balance and recorded as weight W1. The coupon was then suspended in a 100 mL beaker using a glass hook. A 100 mL of 1 M HCl was introduced into reaction beakers. Each coupon was extracted from the test medium at intervals of 3 hours. The corroded coupons were rinsed with bidistilled water and dried using acetone. The coupons were then reweighed, and the final weights, W_2, were recorded. Weight losses, $\Delta W = W_1 - W_2$, were calculated. The inhibition efficiency % IE and surface coverage θ were determined using the following equations:

$$\theta = W_0 - W_i W_0 \quad (1)$$

$$\% IE = W0 - Wi\ W0 \times 100 \quad (2)$$

"Where w_i and w_0 are the weight loss values in the presence and absence of the inhibitor, respectively. The experiment was repeated using various concentrations of (5-EBMB) in the 1 M HCl medium, varying the time between 50 and 180 minutes and the temperature between 25 and 45 °C for a duration of 3 hours. The corrosion rate (k_{corr}) is expressed as an increase in corrosion depth per unit time in (mg cm^{-2} h^{-1}). The corrosion rate equation is given as:"

$$k_{corr}=\Delta W/At \qquad (3)$$

where: ΔW = weight loss of coupon, t = immersion time, and A = area of coupon

2.3. Electrochemical techniques

Electrochemical measurements are taken within traditional three electrodes glass cell include saturated calomel electrode (SCE) linked with fine “Luggin capillary, platinum counter electrode and working electrode is carbon steel with a square cut shape and surface area of 1.0×1.0 cm^2. PDP curves are established through altering the electrode potential automatically from -500 to +500 mV vs. OCP with a sweep rate of 0.2 mVs^{-1}. Stern-Geary method [43] applied the definition of corrosion current is achieved via deducing on cathodic and anodic Tafel lines to a point which provides log i_{corr} and the resulting E_{corr} for 5-EBMB free acid and to any concentration of 5-EBMB”. Thereafter i_{corr} can be applied to examine of θ and IE % as subsequent:

$$IE\% = \theta \times 100 = \left[1 - \frac{i_{corr}}{i_{corr(inh)}}\right] \times 100 \qquad (4)$$

Where, “$i_{corr(free)}$ and $i_{corr(inh)}$ are the corrosion current densities at the absence and existence of 5-EBMB”, separately.

EIS are applied within range of frequency from 100 kHz to 0.01 mHz and 10 mV amplitude peak-to-peak at OCP. The θ and the % IE achieved from the impedance calculation were assessed through the next equation:

$$IE\% = \theta \times 100 = \left[1 - \frac{R^{\circ}_{ct}}{R_{ct}}\right] \times 100 \qquad (5)$$

Where, “R^{o}_{ct} and R_{ct} are the resistance of charge transfer at the absence and existence of 5-EBMB”, separately.

EFM tests were accomplished via dual frequencies “2 and 5 Hz with base frequency 0.1 Hz, consequently the wave shape repeats subsequently at 1s. The large peaks located in the intermodulation spectra were utilized to assess the corrosion current density (i_{corr}), the Tafel slopes (β_a and β_c) and CF-2 & CF-3” [44, 45], the %IE and θ were assessed from Eq. (2).

All electrochemical experiments are ready solution at 25 ±1°C. The potential of electrode can be permitted until become stable 30 min prior to start the measurements. All electrochemical experiments were done at 25±1°C and accomplished via Gamry (PCI4/ 750G) Potentiostat/Galvanostat/ ZRA. This includes Gamry Framework for controlling and Echem Analyst5.58 software for data analysis and plotting.

3. RESULTS AND DISCUSSION

3.1. WL method

The WL-time diagrams for the corrosion of C-steel in 1 M hydrochloric solution before and after addition of diverse concentrations of 5-EBMB is displayed within Fig. 1. This Figure demonstrates that the values of WL for C-steel with 1M hydrochloric acid solution lies higher than in 5-EBMB and the WL decreases as 5-EBMB dose rises; It is meaning the strengthens of corrosion inhibition by increasing the 5-EBMB concentration as listed in Table 2. This explains the adsorption of 5-EBMB molecules on the C-steel surface, i.e., the C-steel surface is shielded from the aqueous media through creation of protecting film on this surface [46, 47].

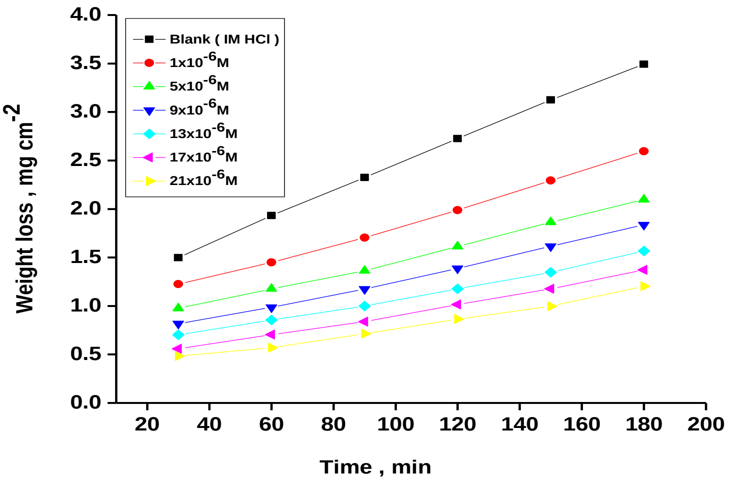

Figure 1. Time-WL bends for C-steel in 1M HCl in the absence and presence of diverse doses of 5-EBMB at 25 ºC

Table 2. Variation of % IE with altered doses of investigated 5-EBMB at 25oC from WL measurements at 120 min dipping in 1.0 M HCl

Conc. (M)	k_{corr} (mg cm^{-2} min^{-1})	% IE
Blank	0.028	---
1x10^{-6}	0.022	47.1
5x10^{-6}	0.017	55.8
9x10^{-6}	0.015	58.1
13x10^{-6}	0.013	62.7
17x10^{-6}	0.011	68.6
21x10^{-6}	0.009	74.7

3.2. PDP studies

Figure 2 illustrates the Tafel polarization diagrams for C-steel in 1 M hydrochloric acid in the absence and existence of 5-EBMB dose at 25oC, separately. From Fig.2, it is obvious that anodic metal dissolution and cathodic H2 reduction reactions were controlled when 5-EBMB was added to 1 M HCl solution also this inhibition was more obvious through raising the dose of the 5-EBMB. The computation of icorr is made possible by the extrapolation of Tafel straight lines. Table 3 lists the values of icorr, the corrosion potential Ecorr, θ, and the percentage of IE as well as the cathodic and anodic Tafel slopes ($β_a$, $β_c$). Table 3 illustrates that i_{corr} declines via addition of the 5-EBMB and through raising its doses. Additionally, it is evident that, in the presence of different dosages of 5-EBMB in a 1 M HCl solution, there is no discernible trend in Ecorr values (15 mV). According to this finding, 5-EBMB in a 1 M HCl solution can be categorized as a mixed-type inhibitor [48, 49]. Furthermore, Tafel slopes [βa, βc] remain nearly constant, suggesting that the adsorption of 5-EBMB alters both the cathodic hydrogen evolution and anodic dissolution mechanisms. [50,51].

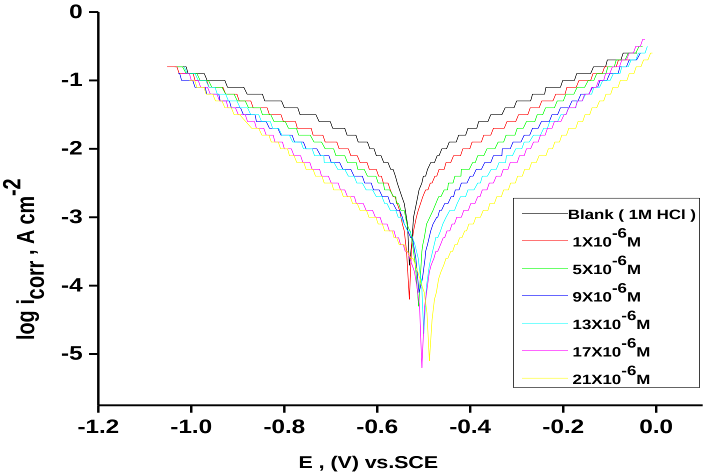

Figure 2. PDP diagrams for dissolution of C-steel in 1M HCl in the attendance and absence of altered doses of 5-EBMB at 25 ºC.

Table 3. Corrosion parameters of C-steel electrode in 1M HCl solution containing altered doses of 5-EBMB at 25℃ from PP technique

Conc., x10^{6} M	-E_{corr} (mV , vs. SCE)	i_{corr} (mA cm^{-2})	- $β_c$ mV dec $^{-1}$	$β_a$ mV dec $^{-1}$	θ	%IE	k_{corr} mmy^{-1}
1 M HCl	587	422	42	22	---	---	220.6
1x10^{-6}	585	369	37	36	0.378	37.8	186.5
5x10^{-6}	584	263	61	42	0476	47.6	120.1
9x10^{-6}	583	206	71	51	0.579	57.9	94.3
13x10^{-6}	580	160	80	58	0.685	68.5	73.3
17x10^{-6}	573	123	64	46	0.757	75.7	56.2
21x10^{-6}	572	96.8	122	82	0.825	82.5	44.2

3.3. EIS studies

Utilizing the EIS approach, the electrode/ electrolyte interface and the corrosion processes on the C-steel surface were examined in both the presence and absence of 5-EBMB. EIS measurements in a broad frequency range at 25 °C were conducted at OCP to guarantee thorough characterization of the interface and surface processes. The impact of the doses of 5-EBMB on the impedance of C-steel in 1M HCl at 25 ºC is produced in Nyquist and Bode plots as shown in Fig. 3 a, b. Curves show identical kind of Nyquist bends for C-steel with existence of diverse doses of 5-EBMB. Presence of single semi-circle displayed the single charge transfer procedure through dissolution which is unaltered with the existence of 5-EBMB compound. Deviations from ideal circular form are frequently signalize to the frequency dispersal of impedance interfacial which occurs because of impurities, surface coarseness, grain limits, dislocations, forming of porous layers and adsorption of derivatives, also homogenized on the surface of electrode [52,53]. Observation of these data detected from all impedance graphs contains of large capacitive circle by only time constant of capacitive with Bode–phase graphs (Fig.3b). The electrical equivalent circuit is displayed in Fig. 4 and it applied for examine achieve impedance data.

This circuit involves R_{ct} (The corrosion rate is inversely related to the Rct value, which measures electron transmission over the surface) , C_{dl} also the solution resistance (R_s). Fit excellent through this model can be gained through experimental data. EIS outcomes in Table 4 distinguished that C_{dl} values declines as well as R_{ct} values rises by rising doses of 5-EBMB. It is because of the increasing in the thickness of the adsorbed layer and to the exchange of the adsorbed water molecules with the 5-EBMB molecules on the surface of metal, declining the metal dissolution reaction [54, 55]. The diminishing in C_{dl} can be caused by a drop in the local dielectric constant and/or a rise in the thickness of the double layer electrical suggested that 5-EBMB molecule function through adsorption at the metal and solution interface [56]. Using the chi-squared approach, the accuracy of the fitted results was assessed; each result's minuscule chi-squared value (Table 4) shows that the fitted results and the experimental findings are in close agreement. The %IE gained from EIS studies are close to those inferred of PDP studies.

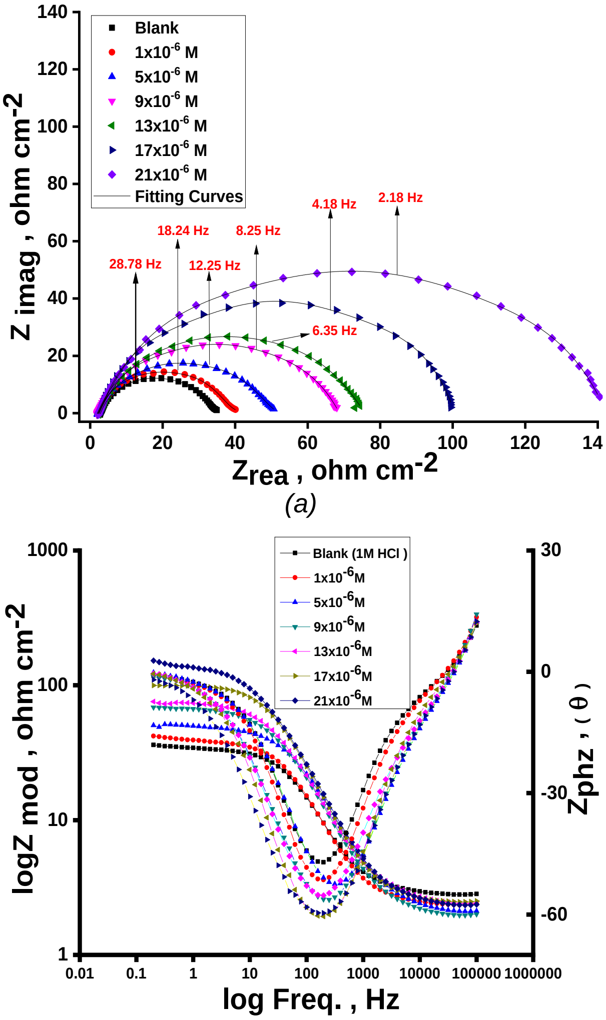

(a)

(b)

Figure 3. Nyquist plots (a) and Bode plots (b) for C-steel in 1M HCl at different concentrations of 5-EBMB at 30⁰C

Table 4. EIS data of C-steel in 1M HCl and in existence of altered doses of 5-EBMB at 25ºC

Conc., M	Yo, μΩ−1 sn cm^{-2}	n	Cdl (μF cm^{-2})	Rct, (ohm cm^{2})	θ	%IE	Goodness of fit, (χ2)
1M HCl	129	0.995	117	31.7	---	---	17.24x10^{-3}
1x10^{-6}	118	0.989	102	37.5	0.147	14.7	13.25x10^{-3}
5x10^{-5}	103	0.984	92	47.8	0.339	33.9	14.15x10^{-3}
9x10^{-5}	97	0.981	86	66.1	0.521	52.1	12.54x10^{-3}
13x10^{-6}	88	0.976	79	72.5	0.563	56.3	16.47x10^{-3}

$17x10^{-6}$	86	0.968	77	97.7	0.676	67.6	$17.87x10^{-3}$
21x10-6	74	0.961	69	139.7	0.773	77.3	12.53x10-3

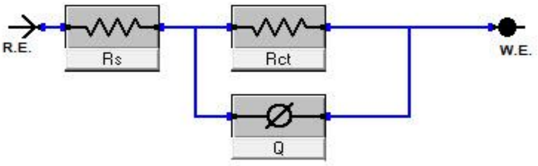

Figure 4. Electrical equivalent circuit model utilized to fit the results of impedance

3.4. EFM studies

EFM spectra intermodulation for C-steel in 1 M hydrochloric acid solution before and after adding $21x10^{-6}$M of 5-EBMB is displayed in Fig. 5. The bigger peaks were applied to examine i_{corr}, β_c, β_a, CF-2 and CF-3. Those electrochemical factors are concurrently specified then recorded in Table 5.

It can be viewed from this Table 5, the values of i_{corr} diminish with existence of various doses of 5-EBMB than with existence only of 1 M HCl in situation of C-steel. The obtained Causality factors for the examined data are in excellent quality with their theoretical (2 &3) values.

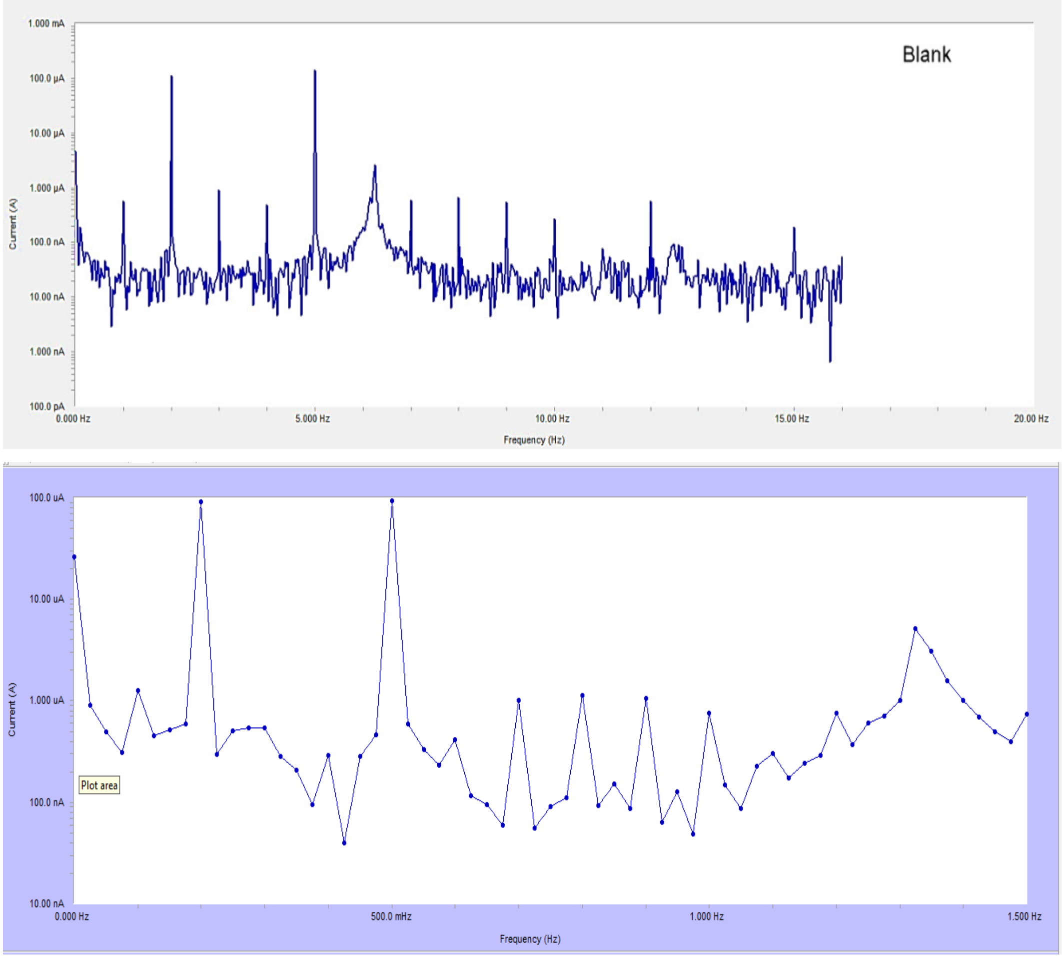

Figure 5. EFM spectra for C–steel in 1M HCl with and without $21x10^{-6}$ M of 5-ABA at 25°C

Table 5. EFM parameters for C-steel 1M HCl solution and existence of altered doses of 5-EBMB at 25°C

Conc., (M)	i_{corr}, (μA cm^{-2})	β_1,(mVdec^{-1})	β_2, (mVdec^{-1})	CF-2	CF-3	k_{corr}, mmy^{-1}	% IE
1M HCl	808.5	113	164	2.09	1.75	370.2	---
$1x10^{-6}$	599.9	99	137	2.04	3.23	274.1	25.8
$5x10^{-6}$	453.9	101	126	1.95	3.09	207.4	43.9
$9x10^{-6}$	374.5	112	118	2.05	3.08	172	53.7
$13x10^{-6}$	272.7	97	101	1.73	2.61	124.6	66.3

$17x10^{-6}$	233.1	92	118	1.97	2.57	106.5	71.2
$21x10^{-6}$	152.6	105	111	1.49	1.83	69.7	81.1

3.5. Effectiveness of temperature

Temperature impact on the rate of corrosion of C-steel in 1 M HCl including diverse concentration of the investigated 5-EBMB can be examined via WL method at temperature ranges of 25 to 55°C (Table 6). The Outcomes discovered that, by raising the temperature the rate of corrosion rises and decline with dose of the 5-EBMB rise for the investigated 5-EBMB.

Table 6. Data of WL measurements for C-steel in 1M HCl solution with and without altered doses of 5-EBMB at 25 – 55°C

Conc. (M)	Temp. (°C)	k_{corr} (mg cm^{-2} min^{-1})	θ	% IE
Blank (1 M HCl)	25	0.028	----	----
	35	0.033	----	----
	45	0.039	----	----
	55	0.045	----	----
$1x10^{-6}$	25	0.022	0.249	47.1
	35	0.026	0.196	19.6
	45	0.033	0.149	14.9
	55	0.038	0.137	13.7
$5x10^{-6}$	25	0.017	0.394	55.8
	35	0.022	0.314	31.4
	45	0.028	0.258	25.8
	55	0.033	0.242	24.2
$9x10^{-6}$	25	0.015	0.471	58.1
	35	0.019	0.405	40.5
	45	0.025	0.339	33.9
	55	0.030	0.315	31.5
$13x10^{-6}$	25	0.013	0.558	62.7
	35	0.017	0.475	47.5
	45	0.022	0.416	41.6
	55	0.026	0.403	40.3
$17x10^{-6}$	25	0.011	0.627	68.6
	35	0.014	0.554	55.4
	45	0.019	0.495	49.5
	55	0.023	0.479	47.9
$21x10^{-6}$	25	0.009	0.683	74.7
	35	0.012	0.627	62.7
	45	0.017	0.563	56.3
	55	0.020	0.555	55.5

The activation energy (E^*_a) can be examined by applying Arrhenius equation:

$$k = A\, e^{\frac{-E_a^*}{RT}} \tag{6}$$

Where

A is Arrhenius constant and k is rate of corrosion. Straight lines are displayed in Fig. 6.and their linear regression (R^2) is nearer to 1 and E^*_a can be obtained from the slope. Table 6 displayed that the value of E^*_a for uninhibited solution is lower than inhibited solution, supposing that the dissolution of C-steel is slow within existence of 5-EBMB [57]. This is recognized from Eq. 10 the higher values of E^*_a cause lower corrosion rate owing to construction of protecting film on the C-steel surface acting as an energy barrier of the C-steel corrosion [58-60]. Entropy and enthalpy of activation (ΔS^*, ΔH^*)" of the corrosion procedure were reckoned from the transition state theory:

$$k=\left[\frac{RT}{Nh}\right]e^{\frac{\Delta S^*}{R}}e^{\frac{-\Delta H^*}{RT}} \qquad (7)$$

Where

N Avogadro's number and h Planck's constant. The graphs of log k/T versus 1/ T of C-steel with 1 M hydrochloric acid solution at diverse doses from examined compound, provides straight lines as displayed in Fig.7 for 5-EBMB. The thermodynamic parameters are list in Table 6 shows that ΔH* values are positive signalize that the steel dissolution process is endothermic process. High and negative values of ΔS* assume that activated complex found in an association form more than dissociation form.

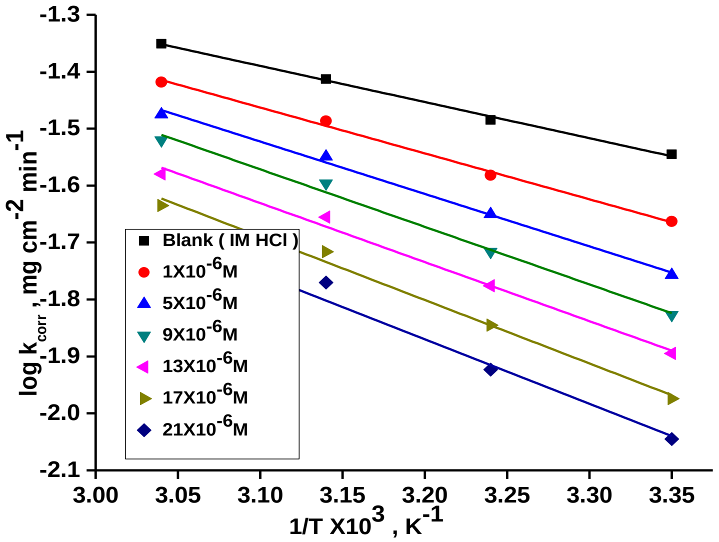

Figure 6. Log k_{corr} – 1/T curves for C-steel dissolution in 1.0 M HCl in the absence and existence of altered doses of 5-EBMB

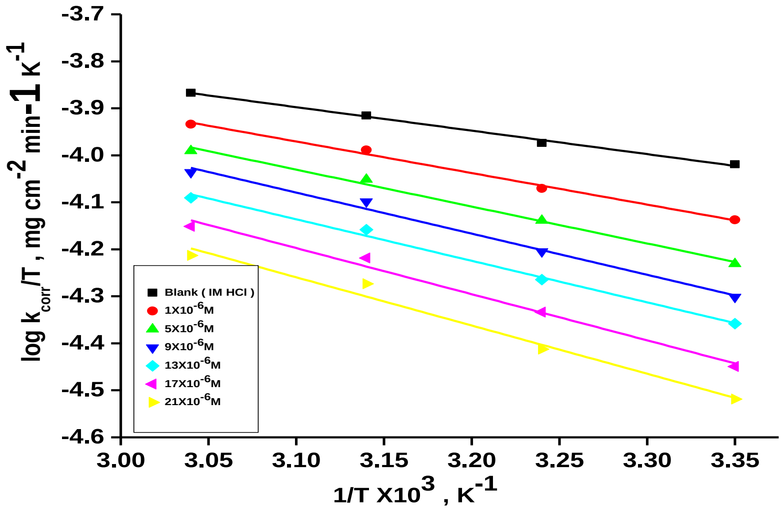

Figure 7. log k_{corr}/T – 1/T curves for C-steel dissolution in 1M HCl and existence of altered doses the investigated 5-EBM

Table 7. Activation parameters for dissolution of C-steel in the absence and existence of altered doses of 5-EBMB in 1M HCl

Activation parameters				
Conc. M	E_a^*, kJ mol^{-1}	ΔH*, kJ mol^{-1}	ΔS*,- J mol^{-1}K^{-1}	Regression Coefficient, (R^2)
Blank	12.2	9.6	108.6	0.9941
1x10^{-6}	15.4	12.8	99.8	0.9921
5x10^{-6}	17.6	15.1	94.1	0.9917
9x10^{-6}	19.3	16.8	89.7	0.9868

$13x10^{-6}$	19.9	16.9	90.3	0.9907
$17x10^{-6}$	21.3	18.8	85.7	0.9845
$21x10^{-6}$	21.7	19.6	84.2	0.9718

3.6. Adsorption Isotherm

Organic compounds are inhibited the metal corrosion through adsorption on surface of metal. The adsorption procedure is considered as single replacement process of adsorbed water molecules (x) by a single 5-EBMB molecule [61,62].

$$I_{(aq)} + xH_2O_{(sur)} \rightarrow I_{(sur)} + xH_2O_{(aq)} \qquad (8)$$

As well, the adsorption affords data about interaction between the adsorbed molecules and the surface of metal. The values of θ for diverse doses of the analyzed 5-EBMB at various temperatures have been applied to describe the most suitable adsorption isotherm to define adsorption procedure. Results of the studied derivative are suitable with Langmuir adsorption isotherm**. Fig 8** displays the plotting of C/θ versus C at 25°C to examine 5-EBMB, separately. Those schemes provided straight lines with unit slope signalized that adsorption of 5-EBMB on C-steel surface confirmed Langmuir equation [63].

$$\frac{C}{\theta} = \frac{1}{K_{ads}} + C \qquad (9)$$

where, “C is the 5-EBMB concentration and K_{ads} is adsorption equilibrium constant” associated to the free energy of adsorption ΔG_{ads} as appear [64]:

$$K_{ads} = \frac{1}{55.5} e^{\frac{-\Delta G^{\circ}_{ads}}{RT}} \qquad (10)$$

where, “T is the absolute temperature R is the universal gas constant and 55.5 is the concentration of water on the metal surface in M”. The K_{ads} and ΔG^o_{ads} values of 5-EBMB are 2,.08 x 10-5 M-1 and 40.3 kJ mol-1, respectively. The increase in the negative value of ΔG^o_{ads} indicates that the 5-ABA was strongly adsorbed onto the C-steel surface in a stable state and that the adsorption process was spontaneous. From this data the adsorption of 5-EBMB on C-steel on C-steel surface is mixed type i.e., physisorption and chemisorption, but mainly physisorption because the E^*_a values increases in presence of 5-EBMB than in its absence and % inhibition decreases by raising temperature [65].

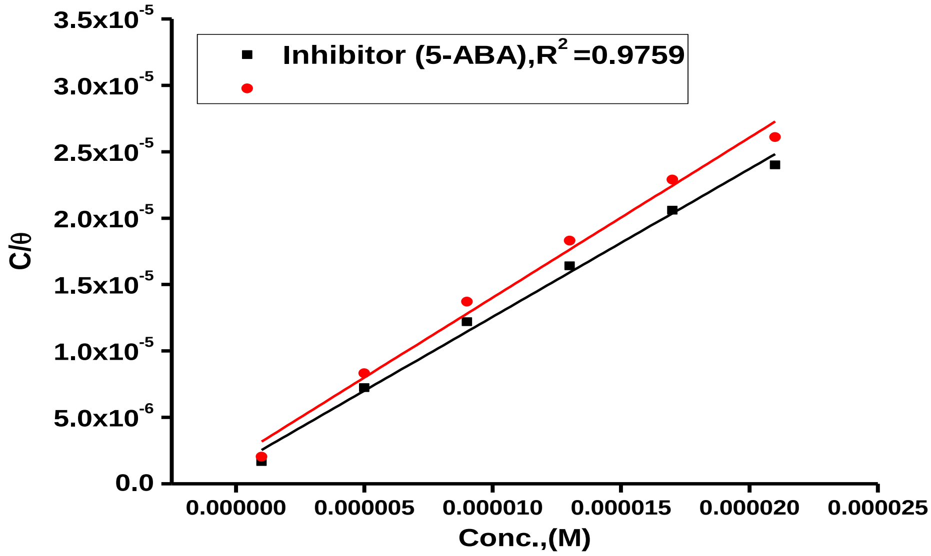

Figure 8. Langmuir isotherm plots for C-steel in 1 M HCl containing various doses of 5-EBMB at 25 °C

3.7. Surface Examination

3.7.1. SEM & EDX analysis

Figure (9a,b) describes the C-steel samples in 1M HCl acid in the lack and existence of 21×10^{-6} M 5-EBMB. The SEM image after C-steel exposure to 1 M HCl for 24 h, was severely scratched and destroyed (Fig. (9a) whereas, after adding the optimum dose of 5-EBMB the surface turns smoother and free slightly from corrosion product this presumed the protection action of inhibitor via restraining the active centers of the C-steel surface. Fig. (9 c, d) implies the EDX analysis and the percentage of atomic content of blank and inhibited pieces, respectively. The strong Fe signal (Fig. 9d) implied a Fe-rich pristine C-steel surface. However, untreated C-steel surface exposed to 1M HCl as a corrosive medium exhibited O, Cl, and Fe signals (Table Fig. 9a). This might be related to strong corrosion and/or formation of iron chloride and/or iron oxide layers on the CS surface. As revealed in (Fig. 9c, d) the EDX spectrums of 5-EBMB display additional signals due to the occurrence of N and O.

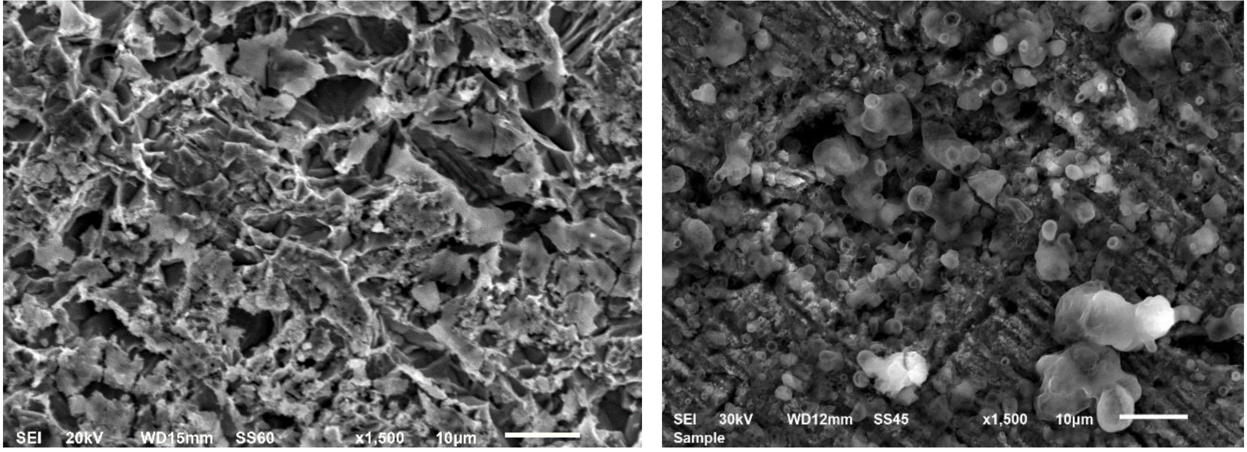

(a) Blank *(b) Compound 5-EBMB*

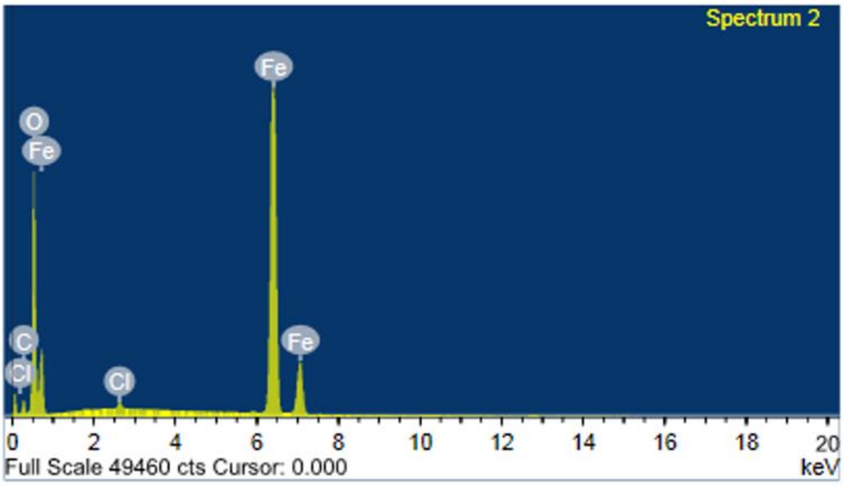

(c) Blank

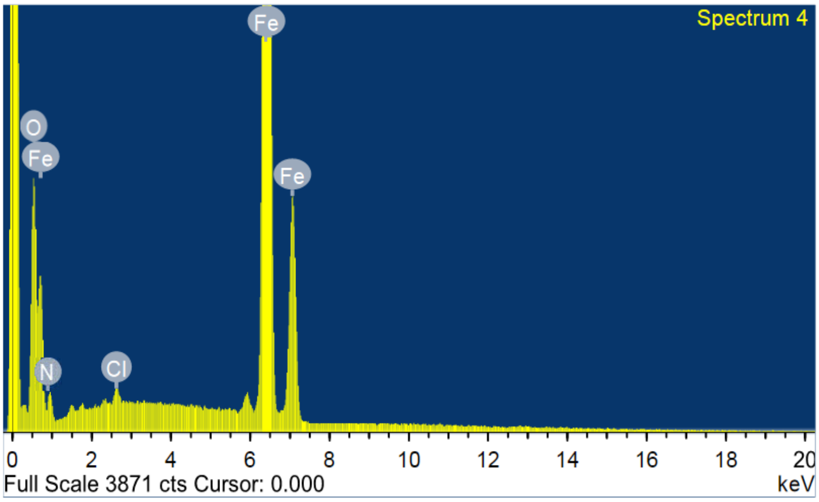

(d) Compound 5-EBMB

Figure 9. SEM images and EDX spectra of the C-steel surface before and after immersion in 1 M HCl in the lack and existence of 21×10^{-6}M for 5-EBMB 24 h at 25°C

The occurrence of N and O elements in the EDX models of inhibited surface determines the inhibitor molecule is adsorbed on the C-steel interface and inhibiting from corrosion (Table 8).

Table 8. Atomic content percentage of the C-steel surface prior and after submersion in 1 M HCl in the lack and existence of 21×10^{-6}M of 5-EBMB for 24 h at 25°C

Atomic content %	Fe	C	Cl	O	N
Free	92.16	7.84	--	--	--
Blank	63.05	11.69	2.35	22.91	--
5-EBMB	70.21	11.33	2.19	15.95	0.32

3.7.2. AFM analysis

AFM is one the most powerful method which used to detect the effect of 5-EBMB on CS surface by studying the morphology of the surface. CS surface was prepared before starting this examination by polishing its surface and immersion of CS pieces in HCl solution for 24 hrs in existence and nonexistence of 21×10^{-6} M of 5-EBMB **[42].** Topographic maps of CS surface are represented in Fig. 10 where 2D and 3D images were appeared. R_q (square roughness) and Ra (average roughness). R_a has a small value in presence of 5-EBMB (115.2 nm) and its value is high in case of C-steel in HCl only (161.8 nm). R_q is 179.5 nm, 150.6 nm without and with 5-EBMB, respectively.

3.8. Theoretical calculations

3.8.1. DFT studies

In the aqueous phase, the optimal structure, HOMO, and LUMO distribution of 5-EBMB molecules are revealed in Fig. 10, and the quantum chemical characteristics are included in Table 9.

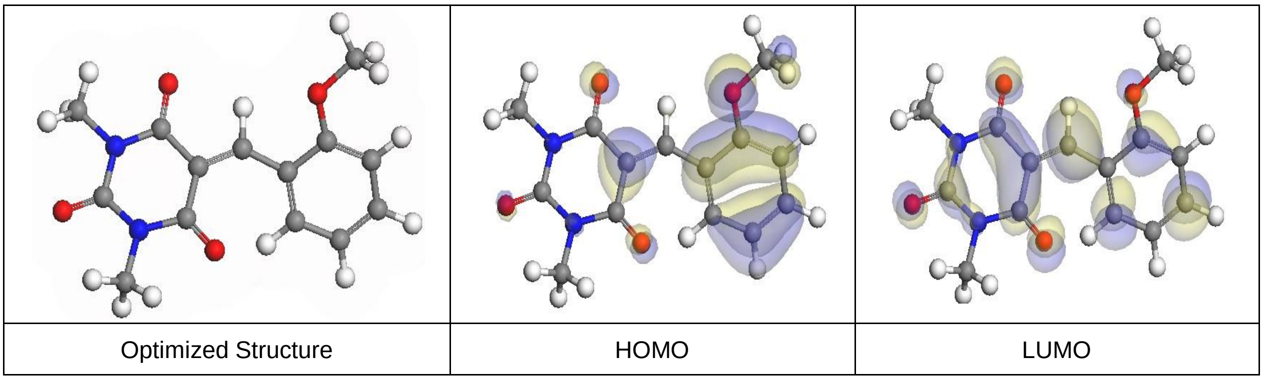

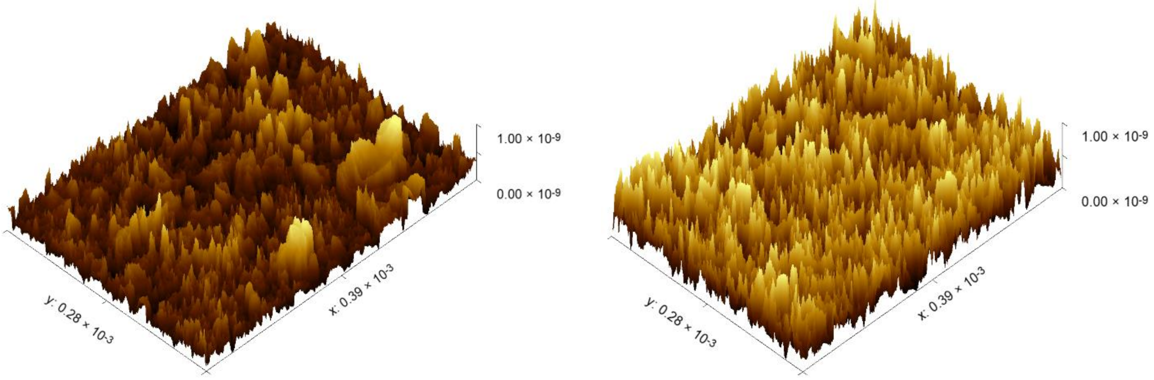

(a) Blank *(b) 5-EBMB*

Figure 10. The optimized molecular structures, HOMO and LUMO for the utilizing DFT caculations in the aqeous phase for 5-EBMB inhibitor

Fig. 10 represents the energy diagram of the Frontier molecular orbitals for the investigated compound and its assessed ΔE. The interaction between the inhibitor molecule and the metal is directed by HOMO and LUMO energies, according to the Frontier orbital theory [66[. Where E_{HOMO} signifies the capability of a molecule to contribute electrons and E_{LUMO} signifies the capacity of a molecule to receive electrons [67]. As a result, the corrosion inhibition capability of an inhibitor molecule with high E_{HOMO} and low E_{LUMO} values improves. Similarly, high corrosion protection efficiency was proposed for an inhibitor molecule with a low energy gap between LUMO and HOMO energy (ΔE) since proffering an electron from E_{HOMO} to E_{LUMO}. According to Table 9, 5-EBMB has larger E_{HOMO} value of -5.47 eV. As exposed in Fig. 10, for the 5-EBMB molecules, we notice that the HOMO level is identified on the phenyl, methoxy and pyrimidine moieties, implying that the O and N atoms are the desired location for electrophilic attacks on the surface of C-steel. This would enhance the adsorption capability of 5-EBMB molecules on the C-steel surface and therefore enhance the protection efficiency, which is in an excellent concurring with the empirical results. Moreover, the E_{LUMO} values are -5.47 eV for 5-EBMB (Table 9) indicating the great inhibition efficacy for 5-EBMB. Similarly, the energy gap (ΔE) is another critical aspect in approving the inhibitor molecule's corrosion prevention capability, which improves as the (ΔE) value decreases [68]. 5-EBMB exhibits lower (ΔE) values (2.66 eV), as shown in Table 9, indicating a higher propensity for 5-EBMB to be adsorbed on the C-steel surface.

Table 9. Calculated quantum chemical parameters for the structure of 5-EBMB in the aqueous phase

Compound	5-EBMB
E_{HOMO}, eV	-5.47
E_{LUMO}, eV	-2.81
ΔE, eV	2.66
I, eV	5.47
A, eV	2.81
χ, eV	4.14
η, eV	1.33
σ, eV	0.75
ΔN, e	1.08
Dipole moment, Debye	6.42
Molecular surface area, Å^2	289.05

Furthermore, because of the low electronegativity (χ), the 5-EBMB molecules have a high potential reactivity to offer electrons to the metal surface [69]. Furthermore, the global hardness η and softness σ of a molecule are important qualities that determine its consistency and reactivity. Because electrons are smoothly afforded to the C-steel surface via adsorption, soft molecules are more reactive than hard molecules [70]. The ΔN values determine the electron contributing capability of the inhibitor, and the higher the ΔN value, the larger the electron providing facility of the inhibitor molecule. According to Lukovits's study [71], when ΔN < 3.6, the % IE improves with greater electron donating ability. The calculated values of ΔN are listed is 1.08 eV. This means that 5-EBMB molecule has greater proclivities to offer electrons to the surface of C-steel. Furthermore, the dipole moment is an important indicator for forecasting the path of corrosion protection [72].The augmentation in dipole moment leads to an increase in deformation energy and better molecule adsorption on steel surface, enhancing inhibitory activity [73]. 5-EBMB has a greater dipole moment value (6.42 debye), as shown in Table 9, indicating a strong tendency for 5-EBMB to be adsorbed on the C-steel surface and enhance inhibition effectiveness. Furthermore, the molecular size of the 5-EBMB and its tendency to protect C-steel surface in corrosive environment has a clear relationship. The inhibition efficiency upsurges with increasing of the molecular structure size because the contact area between the inhibitors molecules and the steel surface raises [74]. As mentioned in Table 10, 5-EBMB demonstrates the greater area (289.05Å^2) and for this purpose, it has greater inhibition proficiency. MEP mapping is a powerful 3D vision tool for distinguishing the net electrostatic effect established over a molecule from total charge dispersal [75]. The red colors in Fig. 11 signify the highest electron density, with MEP being the biggest negative (nucleophilic reaction). The blue colors, on the other hand, signify the most positive region (electrophilic reaction) [76]. The largest negative (red color) regions in methoxy and pyrimidine moieties are generally over N and O atoms, whereas the lower density (yellow color) regions in 5-EBMB molecules are mostly over phenyl moieties. In keto form, MEP, on the other hand, showed the most positive (blue hue) area over oxygen". "The locations in 5-EBMB molecules with the highest electron density may be the furthermost proper for interactions with the C-steel surface".

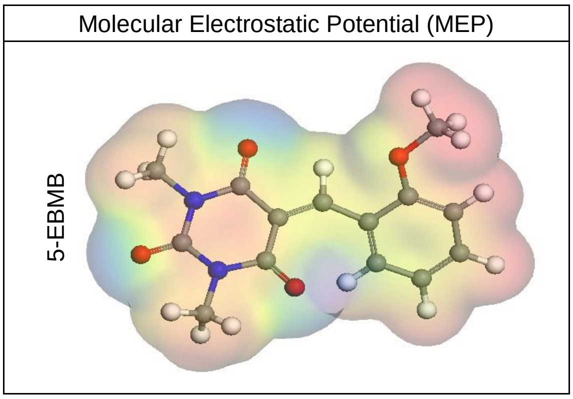

Figure 11. Graphical presentation of the MEP for the 5-EBMB utilizing DFT caculations in the aqeous phase

3.8.2 Monte Carlo (MC simulation)

"MC simulations are theoretical approaches for comprehend the nature of the interaction between the 5-EBMB molecules and the C-steel surface thru the adsorption procedure by retaining the adsorption locator module". Therefore, "Fig. 12

divulges the highest appropriate adsorption configurations for the 5-EBMB molecules on the C-steel surface which located in nearly parallel or flat disposition, designating an increase in the scope of adsorption and greatest surface coverage” [77]. “Table 10 also lists the results of the Monte Carlo simulation, including the adsorption energy for relaxed adsorbate molecules, the rigid adsorption energy for unrelaxed adsorbate molecules, and the deformation energy for relaxed adorbate molecules” [78]. “Table 10 shows that 5-EBMB (-3467.07 kcal mol^{-1}) has a higher adsorption energy, implying that 5-EBMB has a strong adsorption on the C-steel surface, creating stationary adsorbed layers that protect the C-steel from corrosion, which is concurred with the empirical results”. Furthermore, the findings in Table 10 and after the geometry optimization process, indicating that 5-EBMB have a higher inhibitory efficiency.”When one of the adsorbate is abolished, the dE_{ads}/dN_i values explain the energy of metal-adsorbate conformation”[79]. The dE_{ads}/dN_i value for 5-EBMB (-196.17kcal mol^{-1}) is higher indicating that 5-EBMB molecules have better adsorption molecules. Furthermore, the dE_{ads}/dN_i values for water are close to -14.15 kcal mol-1, which is low indicating that 5-EBMB”molecules have a more durable adsorption than water molecules, indicating that water molecules can be replaced by 5-EBMB molecules”. As a result, the 5-EBMB molecules are forcefully adsorbed on the C-steel surface and form a robust adsorbed defensive layer, resulting in a corrosion shield for the C-steel surface in destructive conditions, as demonstrated by both empirical and theoretical research.

Table 10. Data and descriptors calculated by the Mont Carlo simulation (MC) for the adsorption of the 5-EBMB on iron” (110)

Structures	Adsorption energy/ kcal mol^{-1}	Rigid adsorption energy/ kcal mol^{-1}	Deformation energy/kcal mol^{-1}	dE_{ads}/dN_i: nhibitor kcal mol^{-1}	dE_{ads}/dN_i: Water, kcal mol^{-1}
Fe (110)	-3467.07	-3615.28	148.21	-196.17	-14.15
IV					
Water					

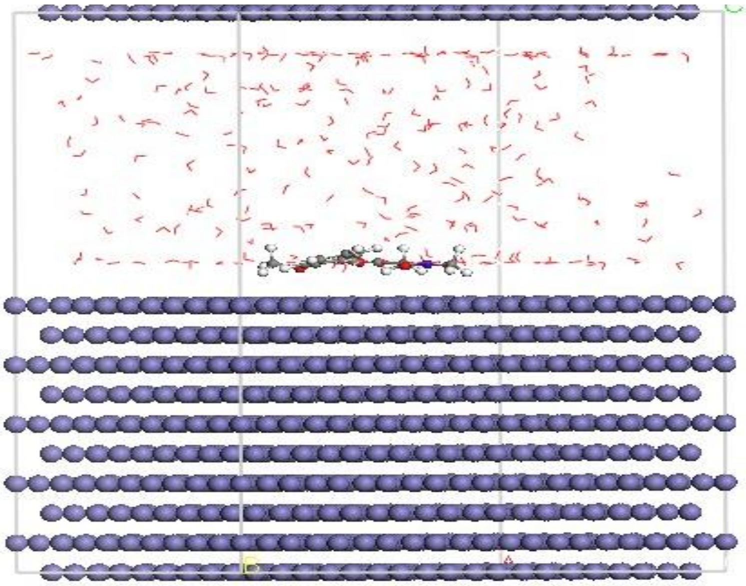

Figure 12. The most appropriate adsorption shape for 5-EBM on Fe (110) substrate obtained from adsorption locator module

4. MECHANISM OF CORROSION AND ADSORPTION

One way to propose an inhibitory mechanism is to employ the inhibitor's adsorption on the steel surface. Because of the complexity involved in both adsorption and inhibition of a particular inhibitor, it is generally not feasible to have a single adsorption mode between the inhibitor and the metal surface. The 5-arylidene barbituric acid derivative (5-EBMB) may adsorb on a C-steel surface's active site in the current system, according to its chemical structure. Consequently, the following adsorption may have an impact on the inhibitory phenomenon:

(i) 5-EBMB can be protonated in an acidic solution due to its neutral O atoms: (5-EBMB) + xH+ → $[5\text{-EBMBH}]^{x+}$ Thus, in acidic solutions, 5-EBMB exist as $[5\text{-EBMB H}]^{x+}$. "They give an excess negative charge in the solution, encouraging cation adsorption since Cl–may adsorb on metal surfaces [80]". A metal surface that is negatively charged could absorb [5-EBMB Hx]$^{x+}$. Stated differently, adsorbed Cl^- and protonated inhibitor may have a synergistic interaction [81].

(ii) 5-EBMB can also be adsorbed on metal surfaces through chemisorption, which strengthens the tension between the inhibitor molecule and the electrode surface by forming coordinate bonds between the lone electron pairs of the O and N atoms and the empty orbital of the Fe atoms. This process occurs in addition to physical adsorption.

(iii) The heterocyclic ring is generally accepted to be the main site of adsorption for heterocyclic compounds. "5-EBMB contains a lot of π-electrons due to the heterocyclic ring, and these electrons may be adsorbed on the metal surface due to donor–acceptor interactions between the unoccupied d-orbitals of Fe and the π-electrons of the heterocyclic ring."

5. CONCLUSIONS

Researchers also investigated how well this substance, which has a variable chemical makeup, performed in lowering the pace at which C-steel corroded in a 1 M HCl solution at various exposure temperatures (25–45 °C). The above conversation leads to the following conclusions:

1. The inhibitory process increased with rising 5-EBMB concentrations, but it decreased with increasing temperature, according to values from WL measurements.
2. In a 1 M HCl solution, this chemical had a maximum inhibitory performance of 82.5% at a concentration of 2.1×10^{-6} M.
3. The 5-EBMB adhered to the Langmuir adsorption isotherm and had a mixed adsorption nature on the C-steel surface, with physical adsorption predominating.
4. Measurements of potentiodynamic polarization reveal that this substance functions as a mixed-type inhibitor.
5. The charge transfer resistance (R_{ct}) increased and the double layer capacitance values (C_{dl}) decreased at varying concentrations of 5-EBMB, according to the electrochemical impedance spectroscopy data. This is because the inhibitor molecules of 5-EBMB have adsorbed on the metal surface.
6. Theoretical calculations show that the structural characteristics and quantum chemistry parameters, such as energy gap (ΔE), the E_{LUMO}, and chemical softness, are related to the tested drugs' inhibitory efficacy and are compatible with many experimental findings.
7. All of the techniques yielded results that were very consistent with one another.

Acknowledgements

The authors are indebted to Mansoura University for all support and the facilities Provided.

Funding

Open access funding provided by The Science, Technology & Innovation Funding Authority (STDF) in cooperation with The Egyptian Knowledge Bank (EKB).

Competing interests

The authors declare no competing interests

REFERENCE

[1] H.B. Fan, C.-Y. Fu, H.-L. Wang, X.-P. Guo, J.-S. Zheng (2002) Inhibition of corrosion of mild steel by sodium n, n-diethyl dithiocarbamate in hydrochloric acid solution, Br. Corros. J., 37, 122–125.

[2] Y.K. Agrawal, J.D. Talati, M.D. Shah, M.N. Desai, N.K. Shah (2004) Schiff bases of ethylenediamine as corrosion inhibitors of zinc in sulphuric acid, Corros. Sci., 46, 633–651.

[3] G. Trabanelli (1991) Whitney award lecture: inhibitors—an old remedy for a new challenge, Corrosion, 47, 410–419.

[4] D.D.N. Singh, A.K. Dey (1993) Synergistic effects of inorganic and organic cations on inhibitive performance of propargyl alcohol on steel dissolution in boiling hydrochloric acid solution, Corrosion, 49, 594–600.

[5] G. Banerjee, S.N. Malhotra (1992) Contribution to adsorption of aromatic amines on mild steel surface from HCl solutions by impedance, UV, and Raman spectroscopy, Corrosion, 48, 10–15.

[6] S.T. Arab, E.A. Noor (1993) Inhibition of acid corrosion of steel by some S-alkylisothiouronium iodides, Corrosion, 49, 122–129.

[7] A. Frignani, V. Grassi, F. Zanotto, F. Zucchi (2012) Inhibition of AZ31 Mg alloy corrosion by anionic surfactants, Corros. Sci., 63, 29–39.

[8] R.F. V Villamil, P. Corio, S.M.L. Agostinho, J.C. Rubim (1999) Effect of sodium dodecylsulfate on copper corrosion in sulfuric acid media in the absence and presence of benzotriazole, J. Electroanal. Chem., 472, 112–119.

[9] T. Zhao, G. Mu (1999) The adsorption and corrosion inhibition of anion surfactants on aluminium surface in hydrochloric acid, Corros. Sci., 41, 1937–1944.

[10] S.S. Abd El Rehim, H.H. Hassan, M.A. Amin (2001) Corrosion inhibition of aluminum by 1, 1 (lauryl amido) propyl ammonium chloride in HCl solution, Mater. Chem. Phys., 70, 64–72.

[11] I.A. Raspini (1993) Influence of sodium salts of organic acids as additives on localized corrosion of aluminum and its alloys, Corrosion, 49, 821–828.

[12] N. Hajjaji, I. Rico, A. Srhiri, A. Lattes, M. Soufiaoui, A. Ben Bachir (1993) Effect of N-alkylbetaines on the corrosion of iron in 1 M HCl solution, Corrosion, 49, 326–334.

[13] M. Elachouri, M.S. Hajji, S. Kertit, E.M. Essassi, M. Salem, R. Coudert (1995) Some surfactants in the series of 2-(alkyldimethylammonio) alkanol

bromides as inhibitors of the corrosion of iron in acid chloride solution, Corros. Sci., 37, 381–389.

[14] H. Luo, Y.C. Guan, K.N. Han (1998) Inhibition of mild steel corrosion by sodium dodecyl benzene sulfonate and sodium oleate in acidic solutions, Corrosion, 54.

[15] M.A. Migahed, E.M.S. Azzam, A.M. Al-Sabagh (2004) Corrosion inhibition of mild steel in 1 M sulfuric acid solution using anionic surfactant, Mater. Chem. Phys., 85, 273–279.

[16] M.M. Osman, A.M.A. Omar, A.M. Al-Sabagh (1997) Corrosion inhibition of benzyl triethanol ammonium chloride and its ethoxylate on steel in sulphuric acid solution, Mater. Chem. Phys. 50, 271–274.

[17] S.S. Abd El Rehim, H.H. Hassan, M.A. Amin (2003) The corrosion inhibition study of sodium dodecyl benzene sulphonate to aluminium and its alloys in 1.0 M HCl solution, Mater. Chem. Phys., 78, 337–348.

[18] R. Guo, T. Liu, X. Wei (2002) Effects of SDS and some alcohols on the inhibition efficiency of corrosion for nickel, Colloids Surfaces A Physicochem. Eng. Asp., 209, 37–45.

[19] D.P. Schweinsberg, G.A. George, A.K. Nanayakkara, D.A. Steinert (1988) The protective action of epoxy resins and curing agents—inhibitive effects on the aqueous acid corrosion of iron and steel, Corros. Sci., 28, 33–42.

[20] K.R. Ansari, Sudheer, A. Singh, M.A. Quraishi (2015) Some pyrimidine derivatives as corrosion inhibitor for mild steel in hydrochloric acid, J. Dispers. Sci. Technol., 36, 908–917.

[21] G.Y. Elewady (2008) Pyrimidine derivatives as corrosion inhibitors for carbon-steel in 2M hydrochloric acid solution, Int. J. Electrochem. Sci., 3, 1149.

[22] A. Espinoza-Vazquez, G. Negrón-Silva, D. Angeles-Beltrán, M.E. Palomar-Pardavé, M.A. Romero-Romo, H. Herrera-Hernández (2011) Electro-chemical impedance evaluation of uracil and thymine pyrimidine derivatives and its nucleosides compounds as a non-toxic corrosion inhibitors of steels in 1M HCl, ECS Trans., 36, 217.

[23] H. Jafari, K. Sayin, Sulfur containing compounds as corrosion inhibitors for mild steel in hydrochloric acid solution, Trans. Indian Inst. Met. 69 (2016) 805–815.

[24] A. Samide (2013) A pharmaceutical product as corrosion inhibitor for carbon steel in acidic environments, J. Environ. Sci. Heal. Part A., 48, 159–165.

[25] H. Ashassi-Sorkhabi, B. Shaabani, D. Seifzadeh (2005) Effect of some pyrimidinic Shciff bases on the corrosion of mild steel in hydrochloric acid solution, Electrochim. Acta., 50, 3446–3452.

[26] A.S. Fouda, M.A. Ismail, M.A. Khaled, A.A. El-Hossiany (2022) Experimental and computational chemical studies on the corrosion inhibition of new pyrimidinone derivatives for copper in nitric acid, Sci. Rep., 12, 1–19.

[27] S. Lahmidi, A. Elyoussfi, A. Dafali, H. Elmsellem, N.K. Sebbar, L. El Ouasif, A.E. Jilalat, B. El Mahi, E.M. Essassi, I. Abdel-Rahman (2017) Corrosion inhibition of mild steel by two new 1, 2, 4-triazolo [1, 5-a] pyrimidine derivatives in 1 M HCl: Experimental and computational study, J. Mater. Environ. Sci., 8, 225–237.

[28] Z.D. Stanković, M. Vuković (1996) The influence of thiourea on kinetic parameters on the cathodic and anodic reaction at different metals in H2SO4 solution, Electrochim. Acta., 41, 2529–2535.

[29] M.A. El Khalek Khaled, K. Shalabi, M.A. Ismail, F. El Aziz Abd S (2022) Adsorption and inhibitive impact of 5-[4-(dimethylamino) benzylidene]-1, 3-dimethylbarbituric acid on carbon steel corrosion in molar hydrochloric acid solution, Zast. Mater., 63, 238–250.

[30] I. Lukovits, I. Bakó, A. Shaban, E. Kálmán (1998) Polynomial model of the inhibition mechanism of thiourea derivatives, Electrochim. Acta., 43, 131–136.

[31] E.E. Ebenso, U.J. Ekpe, B.I. Ita, O.E. Offiong, U.J. Ibok (1999) Effect of molecular structure on the efficiency of amides and thiosemicarbazones used for corrosion inhibition of mild steel in hydrochloric acid, Mater. Chem. Phys., 60, 79–90.

[32] M.A. Quraishi, F.A. Ansari, D. Jamal (2003) Thiourea derivatives as corrosion inhibitors for mild steel in formic acid, Mater. Chem. Phys. 77, 687–690.

[33] E.G. Brown, E.G. Brown (1998) Pyrimidines, Ring Nitrogen Key Biomol. Biochem. N-Heterocycles, 88–127.

[34] C. Macilwain (1993) Activists now urge caution on approval of new AIDS drug, Nature. 365, 378.

[35] M.A. Khaled, M.A. Ismail, A.A. El-Hossiany, A.S. Fouda (2021) Novel pyrimidine-bichalcophene derivatives as corrosion inhibitors for copper in 1 M nitric acid solution, RSC Adv., 11, 25314–25333.

[36] A. Banan, S. Asadi (2024) Novel cationic and non-ionic biopolyurethanes for effective inhibition of mild steel corrosion in H2S-CO2 environment, Ind. Crops Prod., 221, 119320.

[37] K. Haruna, T.A. Saleh, A. Lawal (2024) Acrylic acid modified indapamide-based polymer as an effective inhibitor against carbon steel corrosion in CO2-saturated NaCl with variable H2S levels: An electrochemical, weight loss and machine learning study, Surfaces and Interfaces, 105065.

[38] H. Bairagi, P. Vashishth, J. Gopal, S.K. Shukla, E.E. Ebenso, B. Mangla (2024) Polymers and their composites for corrosion inhibition application: Development, Advancement, and Future Scope–a critical review, Corros. Commun.

[39] M.A. Ismail, S. Al-Shihry, R.K. Arafa, U. El-Ayaan (2013) Synthesis, antimicrobial activity and molecular modeling study of substituted 5-aryl-pyrimido [5, 4-c] quinoline-2, 4-diones, J. Enzyme Inhib. Med. Chem. 28, 530–538.

[40] K.A. Krasnov, V.G. Kartsev, A.S. Gorovoi (2000) Chemical modification of plant alkaloids. I. Aminomethylation of barbituric acid derivatives by cytisine, Chem. Nat. Compd. 36, 192–197.

[41] G.N. Mu, T. P Zhao, M. Liu, T. Gu (1996) Effect of metallic cations on corrosion inhibition of an anionic surfactant for mild steel, Corrosion, 52.

[42] R.G. Parr, R.A. Donnelly, M. Levy, W.E. Palke (1978) Electronegativity: the density functional viewpoint, J. Chem. Phys., 68, 3801–3807.

[43] A.S. Fouda, S.A.A. El-Maksoud, A. El-Hossiany, A. Ibrahim (2019) Evolution of the corrosion-inhibiting efficiency of novel hydrazine derivatives against corrosion of stainless steel 201 in acidic medium, Int. J. Electrochem. Sci., 14, 6045–6064. https://doi.org/10.20964/2019.07.65.

[44] K. Aramaki, M. Hagiwara, H. Nishihara (1987) The synergistic effect of anions and the ammonium cation on the inhibition of iron corrosion in acid solution, Corros. Sci., 27, 487–497.

[45] A.S. Fouda, E. Abdel-Latif, H.M. Helal, A. El-Hossiany (2021) Synthesis and Characterization of Some Novel Thiazole Derivatives and Their Applications as Corrosion Inhibitors for Zinc in 1 M Hydrochloric Acid Solution, Russ. J. Electrochem., 57, 159–171. https://doi.org/10.1134/S1023193521020105.

[46] J. Aljourani, K. Raeissi, M.A. Golozar (2009) Benzimidazole and its derivatives as corrosion inhibitors for mild steel in 1M HCl solution, Corros. Sci. 51, 1836–1843.

[47] M. Finšgar, J. Jackson (2014) Application of corrosion inhibitors for steels in acidic media for the oil and gas industry: A review, Corros. Sci., 86, 17–41.

[48] A.S. Fouda, R.E. Ahmed, A. El-Hossiany (2021) Chemical, Electrochemical and Quantum Chemical Studies for Famotidine Drug as a Safe Corrosion Inhibitor for α-Brass in HCl Solution, Prot. Met. Phys. Chem. Surfaces, 57, 398–411.

[49] M.A. Migahed, E.M.S. Azzam, S.M.I. Morsy (2009) Electrochemical behaviour of carbon steel in acid chloride solution in the presence of dodecyl cysteine hydrochloride self-assembled on gold nanoparticles, Corros. Sci., 51, 1636–1644.

[50] M.N.H. Moussa, A.A. El-Far, A.A. El-Shafei (2007) The use of water-soluble hydrazones as inhibitors for the corrosion of C-steel in acidic medium, Mater. Chem. Phys., 105, 105–113.

[51] A.S. Fouda, H. Ibrahim, S. Rashwaan, A. El-Hossiany, R.M. Ahmed (2018) Expired drug (pantoprazole sodium) as a corrosion inhibitor for high carbon steel in hydrochloric acid solution, Int. J. Electrochem. Sci., 13, 6327–6346.

[52] E. Bayol, K. Kayakırılmaz, M. Erbil (2007) The inhibitive effect of hexamethylenetetramine on the acid corrosion of steel, Mater. Chem. Phys., 104, 74–82.

[53] O. Benali, L. Larabi, M. Traisnel, L. Gengembre, Y. Harek (2007) Electrochemical, theoretical and XPS studies of 2-mercapto-1-methylimidazole adsorption on carbon steel in 1 M HClO4, Appl. Surf. Sci. 253, 6130–6139.

[54] I. Epelboin, M. Keddam, H. Takenouti (1972) Use of impedance measurements for the determination of the instant rate of metal corrosion, J. Appl. Electrochem., 2, 71–79.

[55] B.B. Damaskin, O.A. Petrii, V.V. Batrakov, E.B. Uvarov, R. Parsons (1971) Adsorption of organic compounds on electrodes, Springer.

[56] A.S. Fouda, M. Eissa, A. El-Hossiany (2018) Ciprofloxacin as eco-friendly corrosion inhibitor for carbon steel in hydrochloric acid solution, Int. J. Electrochem. Sci., 13, 11096–11112. https://doi.org/10.20964/2018.11.86.

[57] S. Da Costa, S.M.L. Agostinho (1989) Electrochemical behavior of copper in 0.5 M H2SO4 solutions in the absence and presence of Fe (III) and benzotriazole, Corrosion, 45, 472–477.

[58] A.S. Fouda, S.E.H. Etaiw, A.M. Ibrahim, A.A. El-Hossiany (2023) Insights into the use of two novel supramolecular compounds as corrosion inhibitors for stainless steel in a chloride environment: experimental as well as theoretical investigation, RSC Adv., 13, 35305–35320.

[59] A.S. Fouda, M.A.A. El-Ghaffar, M.H. Sherif, A.T. El-Habab, A. El-Hossiany (2020) Novel Anionic 4-Tert-Octyl Phenol Ethoxylate Phosphate Surfactant as Corrosion Inhibitor for C-steel in Acidic Media, Prot. Met. Phys. Chem. Surfaces, 56, 189–201. https://doi.org/10.1134/S2070205120010086.

[60] R.W. Bosch, J. Hubrecht, W.F. Bogaerts, B.C. Syrett (2001) Electrochemical frequency modulation: a new electrochemical technique for online corrosion monitoring, Corrosion, 57, 60–70.

[61] H.A. Ali, A.A. El-Hossiany, A.S. Abousalem, M.A. Ismail, A.S. Fouda, E.A. Ghaith (2024) Synthesis of new binary trimethoxyphenylfuran pyrimidinones as proficient and sustainable corrosion inhibitors for carbon steel in acidic medium: experimental, surface morphology analysis, and theoretical studies, BMC Chem., 18, 182.

[62] H. Ashassi-Sorkhabi, N. Ghalebsaz-Jeddi (2005) Inhibition effect of polyethylene glycol on the corrosion of carbon steel in sulphuric acid, Mater. Chem. Phys., 92, 480–486.

[63] K.F. Khaled, N. Hackerman (2003) Investigation of the inhibitive effect of ortho-substituted anilines on corrosion of iron in 1 M HCl solutions, Electrochim. Acta., 48, 2715–2723.

[64] Y. Feng, S. Chen, W. Guo, Y. Zhang, G. Liu (2007) Inhibition of iron corrosion by 5, 10, 15, 20-tetraphenylporphyrin and 5, 10, 15, 20-tetra-(4-chlorophenyl) porphyrin adlayers in 0.5 M H2SO4 solutions, J. Electroanal. Chem., 602, 115–122.

[65] Y.M. Abdallah, K. Shalabi, N.M. Bayoumy (2018) Eco-friendly synthesis, biological activity and evaluation of some new pyridopyrimidinone derivatives as corrosion inhibitors for API 5L X52 carbon steel in 5% sulfamic acid medium, J. Mol. Struct., 1171, 658–671.

[66] S.K. Gupta, R.K. Mitra, M. Yadav, O. Dagdag, A. Berisha, B.B. Mamba, T.T.I. Nkambule, E.E. Ebenso, S.K. Singh (2023) Electrochemical, surface morphological and computational evaluation on carbohydrazide Schiff bases as corrosion inhibitor for mild steel in acidic medium, Sci. Rep., 13, 15108.

[67] G. Gece, S. Bilgiç (2009) Quantum chemical study of some cyclic nitrogen compounds as corrosion inhibitors of steel in NaCl media, Corros. Sci., 51, 1876–1878.

[68] N. Palaniappan, I.S. Cole, A.E. Kuznetsov (2020) Experimental and computational studies of graphene oxide covalently functionalized by octylamine: electrochemical stability, hydrogen evolution, and corrosion inhibition of the AZ13 Mg alloy in 3.5% NaCl, Rsc Adv., 10, 11426–11434.

[69] I.B. Obot, D.D. Macdonald, Z.M. Gasem (2015) Density functional theory (DFT) as a powerful tool for designing new organic corrosion inhibitors. Part 1: an overview, Corros. Sci., 99, 1–30.

[70] D. Romani, S.A. Brandan (2020) Investigating the behaviors of corticosterone hormone in different solvents by using DFT calculations and experimental data, Biointerface Res. Appl. Chem., 10, 4876–4892. https://doi.org/10.33263/BRIAC101.876892.

[71] I. Lukovits, E. Kalman, F. Zucchi (2001) Corrosion inhibitors—correlation between electronic structure and efficiency, Corrosion, 57, 3–8.

[72] I.B. Obot, S. Kaya, C. Kaya, B. Tüzün (2016) Density Functional Theory (DFT) modeling and Monte Carlo simulation assessment of inhibition performance of some carbohydrazide Schiff bases for steel corrosion, Phys. E Low-Dimensional Syst. Nanostructures, 80, 82–90.

[73] K. Shalabi, A.A. Nazeer (2019) Ethoxylates nonionic surfactants as promising environmentally safe inhibitors for corrosion protection of reinforcing steel in 3.5% NaCl saturated with Ca (OH) 2 solution, J. Mol. Struct., 1195, 863–876.

[74] K. Shalabi, O.A. El-Gammal, Y.M. Abdallah (2021) Adsorption and inhibition effect of tetraaza-tetradentate macrocycle ligand and its Ni (II), Cu (II) complexes on the corrosion of Cu10Ni alloy in 3.5% NaCl solutions, Colloids Surfaces A Physicochem. Eng. Asp., 609, 125653.

[75] Y.S. Mary, C.Y. Panicker, M. Sapnakumari, B. Narayana, B.K. Sarojini, A.A. Al-Saadi, C. Van Alsenoy, J.A. War (2015) FT-IR, NBO, HOMO–LUMO, MEP analysis and molecular docking study of 1-[3-(4-Fluorophenyl)-5-phenyl-4, 5-dihydro-1H-pyrazol-1-yl] ethanone, Spectrochim. Acta Part A Mol. Biomol. Spectrosc., 136, 483–493.

[76] S. Ramalingam, P.D.S. Babu, S. Periandy, E. Fereyduni (2011) Vibrational investigation, molecular orbital studies and molecular electrostatic potential map analysis on 3-chlorobenzoic acid using hybrid computational calculations, Spectrochim. Acta Part A Mol. Biomol. Spectrosc., 84, 210–220.

[77] L.H. Madkour, S. Kaya, I.B. Obot (2018) Computational, Monte Carlo simulation and experimental studies of some arylazotriazoles (AATR) and their copper complexes in corrosion inhibition process, J. Mol. Liq., 260, 351–374.

[78] K. Shalabi, A.M. Helmy, A.H. El-Askalany, M.M. Shahba (2019) New pyridinium bromide mono-cationic surfactant as corrosion inhibitor for carbon steel during chemical cleaning: Experimental and theoretical studies, J. Mol. Liq., 293, 111480.

[79] M. Özcan, İ. Dehri, M. Erbil (2004) Organic sulphur-containing compounds as corrosion inhibitors for mild steel in acidic media: correlation between inhibition efficiency and chemical structure, Appl. Surf. Sci., 236, 155–164.

[80] C. Verma, E.E. Ebenso, M.A. Quraishi (2020) Molecular structural aspects of organic corrosion inhibitors: Influence of–CN and–NO2 substituents on designing of potential corrosion inhibitors for aqueous media, J. Mol. Liq., 316, 113874.

[81] M.A. Migahed (2005) Electrochemical investigation of the corrosion behaviour of mild steel in 2 M HCl solution in presence of 1-dodecyl-4-methoxy pyridinium bromide, Mater. Chem. Phys., 93, 48–53.

IZVOD

DOPRINOS INHIBICIJI KOROZIJE UGLJENIČNOG ČELIKA POMOĆU 5-(2-ETOKSIBENZILIDEN) 1,3-DIMETILBARBITURNE KISELINE U RASTVORU HCl: EKSPERIMENTALNA I TEORIJSKA STUDIJA

Inhibirajući uticaj ekološki prihvatljive 5-(2-etoksibenziliden) 1,3-dimetilbarbiturne kiseline (5-EBMB) u 1 M HCl na koroziju ugljeničnog čelika je ispitan metodom gubitka težine (VL), potenciodinamičke polarizacije (PDP), spektroskopija elektrohemijske impedanse (EIS), tehnike elektrohemijske frekvencijske modulacije (EFM). Dobijeni rezultati pokazuju da je proučavana hemikalija dobra 5-EBMB i da, kako u PDP tako iu EIS metodi, njena efikasnost inhibicije (%IE) raste sa povećanjem koncentracije, dostižući 82,5 na 21k10^{-6} M. Nasuprot tome, kada temperatura raste, smanjen je procenat IE. „Adsorpcija ispitivanog derivata na površini C-čelika prati Langmuirovu izotermu. Proces adsorpcije ispitivanog jedinjenja je spontan i smatra se tipom hemisorpcije. PDP krive su pokazale da je proučavani derivat inhibitor mešovitog tipa. Štaviše, rezultati EIS-a su potvrdili da se jedinjenje koje se ispituje adsorbovalo na površini C-čelika podizanjem otpora prenosa naelektrisanja (Rct) na 139,7 ohm cm^{2} i smanjenjem kapacitivnosti dvostrukog sloja (Cdl) sa 102 na 69 µF cm^{-2}. Adsorpcija inhibitora na površini C-čelika je potvrđena ispitivanjem površine primenom mikroskopije atomske sile (AFM), energetski disperzivnog Ks zraka (EDKS) i skenirajuće elektronske mikroskopije (SEM). Pored toga, kvantna hemija i molekularna dinamička simulacija su korišćene da se opširno ispita mehanizam inhibicije korozije 5-EBMB. Sve testirane metode dale su dobru saglasnost.

Ključne reči: *Inhibicija korozije, HCl, C-čelik, derivat ariliden barbiturne kiseline, Langmuirova izoterma*

Naučni rad
Rad primljen: 30.09.2024.
Rad prihvaćen: 20.11.2024.

Mohamed F. Atia: *https://orcid.org/0009-0003-5907-8304*,
Kamal Shalabi: *https://orcid.org/0000-0001-5478-6369*,
Mohamed A. Ismail: *https://orcid.org/0000-0001-5855-3714*,
Abd El-Aziz S. Fouda: *https://orcid.org/0000-0002-3239-4417*
